npj | flexible electronics

www.nature.com/npjflexelectron

ARTICLE OPEN

Check for updates

A compact polymer–inorganic hybrid gas barrier nanolayer for flexible organic light-emitting diode displays

Seung Hun Kim[1]✉, Seung Yong Song[1], Soo Youn Kim[1], Moon Won Chang[1], Hyo Jeong Kwon[1], Kwan Hyuck Yoon[1], Woo Yong Sung[1], Myung Mo Sung[2] and Hye Yong Chu[1]

Atomic layer infiltration technology allows the formation of a nanometer-thick polymer-inorganic hybrid barrier layer in polymer material for flexible organic light-emitting diode (OLED) displays. In this study, according to transmission electron microscopy and secondary-ion mass spectrometry analysis results under various process conditions, a compact polymer-inorganic hybrid nanolayer was successfully formed in a polymer and good barrier performance was revealed with a low water vapor transmission rate under optimal process conditions. Additionally, through gas chromatography-mass spectrometry measurements after ultra-violet radiation testing, polymer out-gassing decreased compared to bare polymers. Based on barrier properties, the polymer with a polymer-inorganic hybrid barrier nanolayer was applied to a flexible OLED display as a substrate. During storage tests and folding tests, the flexible OLED display exhibits good reliability and better flexibility compared to those with an inorganic barrier layer. These results confirm that the polymer-inorganic hybrid nanolayer is suitable for barrier layer formation in flexible OLED displays.

npj Flexible Electronics (2022)6:21 ; https://doi.org/10.1038/s41528-022-00154-y

INTRODUCTION

Water and oxygen have been proven to be mainly responsible for performance degradation in several applications, such as photovoltaic systems, batteries, food packaging, mirco-electromechanical systems, and displays. Therefore, barrier technology for water and oxygen permeation prevention is a key issue and many industry and academic researchers are actively investigating this technology to improve its performance[1–8]. Recently, organic light-emitting diode (OLED) displays, which exhibit high color gamut, fast response time, low power consumption and wide viewing angle compared to other display technologies, were introduced commercially and play an important role in the display field for smartphones, tablets, personal computers, notebooks, and televisions. Furthermore, they are also advantageous owning to their self-emissivity, small thickness, light weight, simplicity, and flexibility, and appear to be ideal candidates for the development of future displays, including foldable, slidable, rollable, wearable and stretchable displays[9–12]. However, due to the use of organic emission layers and metal cathodes, OLED displays are very sensitive to water and oxygen, as well as out-gassing through the environment and the material itself, which causes panel and pixel shrinkage and represents a significant limitation for reliability and commercial applications[13–16]. Therefore, a high barrier performance should be achieved in OLED displays to block water, oxygen and out-gassing.

Generally, OLED displays consist of three main parts: (1) the backplane, which is composed of a thin film transistor(TFT), a metal electrode, and capacitors for driving; (2) the organic emission layer, which includes the anode, cathode, and organic layer for lighting; and (3) the encapsulation for protecting the organic emission layer from environmental elements. In addition, in flexible OLED displays, a polyimide (PI) material is widely used as a substrate for the backplane because of its flexibility, as opposed to glass substrates, and high-temperature stability for TFT fabrication. To use PI as a substrate, high barrier performance for blocking the water and oxygen permeation and low out-gassing through the PI itself should be ensured to achieve the reliability of flexible OLED displays. As PI has poor barrier and blocking properties, typically, an inorganic layer should be deposited on the PI substrate as a barrier layer, which shows a satisfactory barrier performance for current static and high folding-radius flexible OLED displays[17–19]. However, in case of low folding-radius flexible, slidable and rollable OLED displays, the inorganic layer is prone to cracking due to its brittle nature, which in turn decreases its lifetime and causes reliability issues. Therefore, a new barrier technology with more flexibility for water/oxygen permeation and out-gassing prevention is needed and should be developed for future flexible OLED displays.

In previous work, atomic layer infiltration(ALI) technology was proposed as polymer-inorganic hybrid barrier nanolayer formation method using PI as the polymer and Al_2O_3 as the inorganic material. The results showed the feasibility of ALI and the good performance of the hybrid nanolayer as a barrier for water and oxygen[20]. In this work, the barrier properties of the PI-Al_2O_3 hybrid nanolayer for flexible OLED display applications is investigated. For barrier performance assessment, the infiltration characteristics of the PI film with PI-Al_2O_3 hybrid nanolayer via ALI was analyzed through transmission electron microscopy (TEM) and secondary-ion mass spectrometry (SIMS) analysis. Additionally, we measured the permeation and out-gassing properties of the PI-Al_2O_3 hybrid nanolayer through water vapor transmission rate (WVTR) measurements according to various process conditions and gas chromatography-mass spectrometry (GC-MS) measurements after UV radiation testing, respectively. For reliability and flexibility assessment, a flexible OLED display was fabricated using the PI film with the PI-Al_2O_3 hybrid nanolayer as a substrate and evaluated storage test results under high-temperature and humidity conditions and folding test results according to folding radius changes. Finally, the PI-Al_2O_3 hybrid nanolayer was applied

[1]Display Research Center, Samsung Display, Yongin-si, Gyeonggi-do 17113, Republic of Korea. [2]Department of Chemistry, Hanyang University, Seoul 04763, Republic of Korea. ✉email: sh0923.kim@samsung.com

to a commercially available flexible OLED display and its driving characteristic was demonstrated.

RESULTS AND DISCUSSION

Atomic layer infiltration (ALI) technology

Figure 1 shows the ALI process sequence for a polymer material. In general, the ALI process is based on an atomic layer deposition (ALD) process[21]. The ALD process uses the sequential precursors or reactant gas dosing and purging processes, which forms one atomic layer during one cycle. The same sequence is repeated until the target thickness is reached and a thin inorganic layer is deposited on the polymer layer. Otherwise, an exposing step is additionally applied in the ALI process between the dosing and purging processes for precursor and reactant diffusion into a free volume within the polymer, which is the route for water and oxygen permeation, and allows inorganic material to fill the free volume. Finally, the inorganic and polymer materials co-exist and form a polymer-inorganic hybrid nanolayer within the polymer, which becomes a barrier for oxygen and water permeation and out-gassing. This process and related mechanisms are described in detail in our previous work[19]. In this work, an ALI process using trimethylaluminum (TMA) for aluminum and deionized water (DI, H_2O) for oxide was adopted for a 10-μm-thick PI and a PI-Al_2O_3 hybrid nanolayer was formed within the PI. For the ALI process, the process temperature was fixed at 140 °C and the purging process was repeated four times per every purging step with an exposing time of 60 s and a pressure of 1torr using Ar gas. Additionally, the exposing time, exposing pressure, and number of cycles were changed to investigate the properties of the ALI process.

Characteristics of a polymer-inorganic hybrid nanolayer

Figure 2a shows cross-sectional TEM analysis images of the PI-Al_2O_3 hybrid nanolayer according to ALI process conditions. For this experiment, the exposing pressure was fixed at 0.6 torr, while the exposing time and number of cycles were varied from 10 to 200 s and from 5 to 20, respectively. According to the TEM results, by increasing the exposing time, the infiltrated thickness of the PI-Al_2O_3 hybrid nanolayer increased from 29, 30 and 65 Å to 63, 70 and 72 Å for 5, 10 and 20 cycles, respectively. Similarly, by increasing the number of cycles, the infiltrated thickness of the PI-Al_2O_3 hybrid nanolayer increased from 29, 29, 65 and 63 Å to 65, 73, 75 and 72 Å for exposing times of 10, 50, 100 and 200 s, respectively. These results are attributed to an increase in the precursor and reactant diffusion depth into the free volume within the PI as the exposing time and number of cycles increase. It was found that the infiltrated thickness of the PI-Al_2O_3 hybrid nanolayer was saturated at approximately 70 Å. In addition, the diffusion length from one space to another is proportional to the pressure difference; the higher the pressure, the longer the diffusion length[20]. Therefore, in our experiment varying the exposing pressure with an exposing time of 100 s and number of cycles 20, the infiltrated thickness of the PI-Al_2O_3 hybrid nanolayer increased from 53 to 85 Å when the exposing pressure increased from 0.1 to 1 torr, as shown in Fig. 2a. Base on the results above, for PI-Al_2O_3 hybrid barrier nanolayer fabrication via ALI, a sufficient exposing time, exposing pressure and number of cycles are needed and optimal conditions should be considered.

To evaluate the PI-Al_2O_3 hybrid nanolayer composition, SIMS analysis was used, as shown Fig. 2b, and compared to a 500-Å-thich Al_2O_3 inorganic layer formed via ALD on the PI. In these measurements, the ALI process conditions were an exposing time of 100 s and number of cycles 20. In the Al_2O_3 inorganic layer case, high intensities of aluminum and oxygen components co-existed from the initial depth to approximately 500 Å compared to low intensity of carbon component, which represent carbon impurities caused by TMA. After this depth, intensity of carbon component increased sharply, and intensities of aluminum and oxygen components decreased because this area corresponds to the PI layer. Conversely, in the PI-Al_2O_3 hybrid nanolayer case, high intensities of aluminum, oxygen, and carbon components co-existed from the initial depth to approximately 75 Å, which is in agreement with the TEM depth results; in particular, intensity of carbon component was much higher than in the Al_2O_3 inorganic layer case. From these results of the PI-Al_2O_3 hybrid nanolayer case, Al_2O_3 material successfully infiltrated the free volume within the PI material via ALI and makes the PI-Al_2O_3 hybrid nanolayer inner PI.

For the barrier performance investigation, the WVTR was measured using the tritium method[22], which is more precise than the MOCON and Ca tests, with the same ALI process conditions as the SIMS analysis, as shown in Fig. 2c. The WVTR results of the bare PI film and the PI film with the PI-Al_2O_3 hybrid nanolayer were 2.2 $g/m^2 \cdot day$ and 1.4×10^{-5} $g/m^2 \cdot day$, respectively. The latter result is equivalent to that of the current inorganic barrier layer[23] and sufficient for the barrier layer of flexible OLED displays.

The out-gassing characteristics of the hybrid nanolayer formed via the ALI process were investigated through GC-MS system measurements (QP2010 ultra, Shimadzu). The UV radiation test conditions were a power of 1000 W/m^2, humidity of 30–50%, temperature of 100 °C and 15 cycles with an on-time of 16 h and an off-time of 8 h. The GC-MS measurement results are shown in Fig. 3. In general, a polymer in a state where energy is being applied generates various out-gases from dangling bonds, unreacted groups, residues, absorbed gases, among others. Then, these generated out-gases penetrate and discharged to the environment through the free volume of the polymer[24–27]. After the UV radiation test, the bare PI released various organic gases such as 1-Propene, 1,1,3,3,3-pentrafluoro-, acetaldehyde, methyl formate, acetone, acetic acid, formic acid, and 2-butanone, and

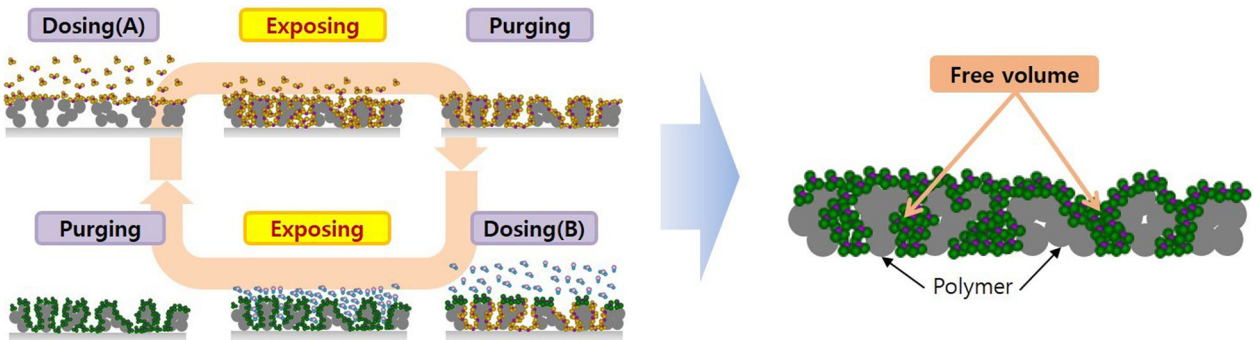

Fig. 1 Atomic layer infiltration. Atomic layer infiltration (ALI) process sequence for polymer-inorganic hybrid nanolayer fabrication by repeating the dosing, exposing, and purging steps.

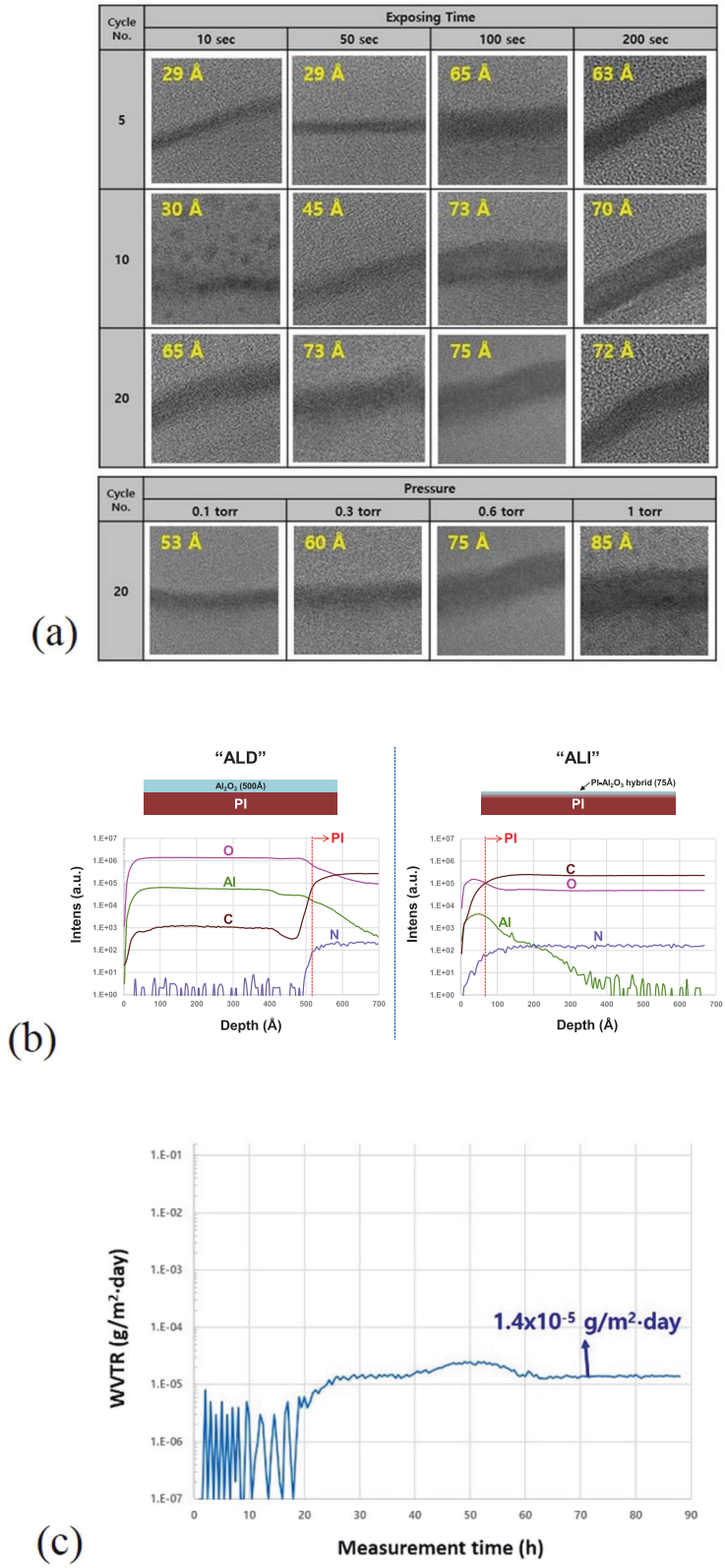

Fig. 2 The results of TEM, SIMS and WVTR. a TEM results according to process conditions. **b** SIMS results for the ALD and ALI processes. **c** WVTR measurement results for the PI-Al_2O_3 hybrid nanolayer.

the total amount of out-gassing was 14,653,472 arbitrary units (A.U.). Conversely, in the PI-Al_2O_3 hybrid nanolayer case under the same conditions, only a small amount of acetaldehyde and acetone were discharged to the environment and the total out-gassing was 374,009 A.U. This result, which is lower than that for the bare PI, is caused by blocking the gas diffusion paths sufficiently infiltrating and filling the free volume within the PI with Al_2O_3.

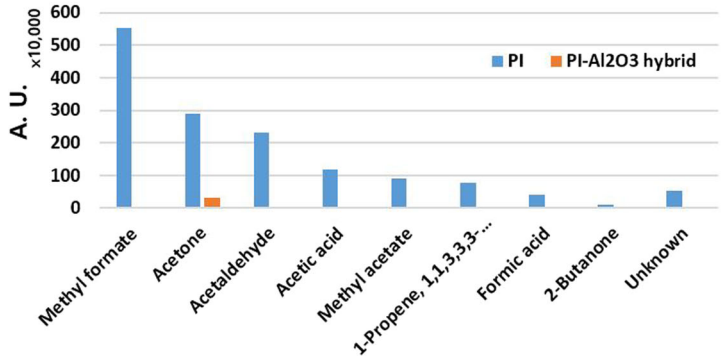

GC-MS	Bare PI	LC PI-Al_2O_3 hybrid
Methyl formate	5,519,788	0
Acetone	2,895,690	322,664
Acetaldehyde	2,298,191	51,345
Acetic acid	1,165,868	0
Methyl acetate	914,513	0
1-Propene, 1,1,3,3,3-pentafluoro-	793,140	0
Formic acid	428,186	0
2-Butanone	100,989	0
Unknown	537,107	0
total	14,653,472	374,009

Fig. 3 The results of GC-MS. Out-gassing results using GC–MS measurements for the bare PI layer and the PI-Al_2O_3 hybrid nanolayer after the UV radiation test.

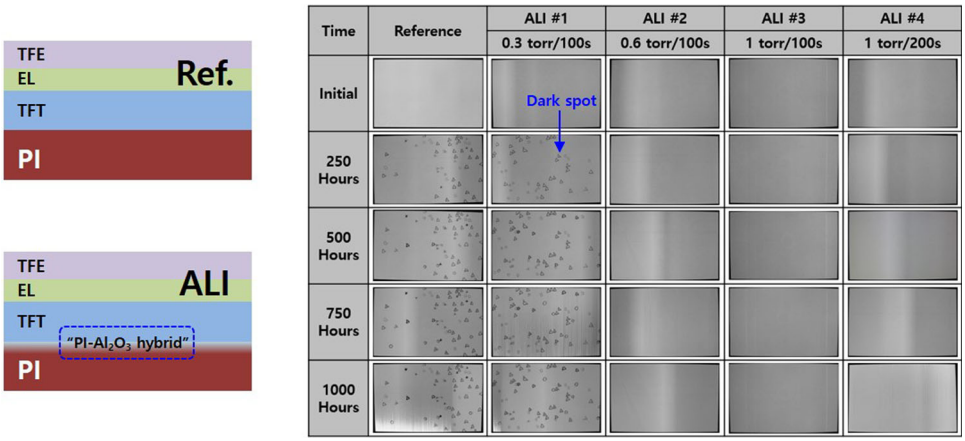

Fig. 4 The results of storage test. Lighting test results for the reliability of the fabricated flexible OLED displays according to ALI process conditions and storage time in a chamber with high temperature (85 °C) and high humid (85% RH).

Reliability and flexibility of flexible OLED displays

Based on the evaluation results of the PI-Al_2O_3 hybrid nanolayer as a barrier, the panel reliability test was adopted for flexible OLED displays. As shown in Fig. 4, various flexible OLED displays were fabricated, one with no barrier layer as the reference and several with the PI-Al_2O_3 hybrid barrier nanolayer applied to the PI substrate. In terms of the ALI process conditions, the exposing pressure was varied from 0.3 to 1 torr and the exposing time from 100 to 200 s while maintaining the number of cycles 20. Then, a low-temperature poly-silicon-thin film transistor (LTPS-TFT), emission layer (EL) and thin-film encapsulation (TFE) were fabricated using various processes, such as PECVD, sputter, photo-lithography, excimer laser annealing, evaporation, and inkjet printing. The fabricated flexible OLED displays were stored in a test chamber with high temperature (85 °C) and high humid (85% RH) for 1000 h, with lighting tests being performed at 250, 500, 750, and 1000 h of storage time for the reliability assessment. The lighting test results are shown in Fig. 4 according to storage time and ALI process conditions with a dark spot marking. As shown in Fig. 4, there are many dark spots in the reference panel after 250 h of storage time because there is no barrier to penetrate the water and oxygen from the outside. In the case of an exposing pressure of 0.3 torr and exposing time of 100 s, many dark spots are also shown after 250 h of storage time because the infiltration is not saturated at a depth of 60 Å, as mentioned in the TEM analysis, and the barrier performance is not sufficient. In contrast, in cases of exposing pressures of 0.6 and 1 torr and exposing times of 100 and 200 s, there are no dark spots until 1,000 h of storage time with a saturated depth of over 70 Å and good WVTR performance. These results indicate that the PI-Al_2O_3 hybrid nanolayer shows a good barrier performance and reliability, making it suitable as a barrier layer for flexible OLED displays.

Additionally, for flexible OLED display applications, the flexibility of the barrier layer is a key characteristic that should be improved. Therefore, folding tests were performed to investigate the flexibility of the PI-Al_2O_3 hybrid barrier nanolayer with a conventional flexible OLED display as reference. Figure 5 shows the structure of flexible OLED displays for testing and folding test results. An inorganic layer using silicon nitride with a thickness of 5,000Å as a reference and the PI-Al_2O_3 hybrid nanolayer were adopted as the PI substrate for the flexible OLED displays. Both barrier layers exhibited a similar WVTR level of approximately 10^{-5} g/m^2 · day. Then, the fabrication processes for the LTPS-TFT, EL, and TFE layers were applied in the same manner as for the reliability test. For the folding test, fabricated flexible OLED displays with two types of barriers were folded in an in-folding direction for 100,000 cycles for various folding radii. After the tests, the normalized WVTR characteristics were measured and compared to that of un-folded flexible OLED display. As shown in Fig. 5, the normalized WVTR in the inorganic barrier case exhibits similar properties according to folding radius, except for that of 1 mm where it increases sharply. These WVTR increase is caused by a crack in the inorganic layer and water permeation through the crack. In the PI-Al_2O_3 hybrid nanolayer case, the normalized

WVTR increased at a folding radius of 0.5 mm but was lower than that of the inorganic layer for all other folding radii. These results show that the PI-Al_2O_3 hybrid nanolayer is more flexible than the inorganic layer and, therefore, more suitable for flexible OLED displays.

Finally, the driving characteristics of the flexible OLED display with the PI-Al_2O_3 hybrid barrier nanolayer were investigated. For this experiment, the flexible OLED display was fabricated with the same structure and processes as the reliability and flexibility evaluation cases. In addition, a flexible printed circuit board (FPCB) and a driving integrated circuit (IC) were implemented to apply a driving signal. Flexible OLED display had the size of 5.77-inch, QHD + resolution (571 ppi), 256 gray scale and RGB diamond pixel shape. As shown in Fig. 6, the flexible OLED display with the PI-Al_2O_3 hybrid barrier nanolayer shows normal operation compared to the conventional OLED display. In addition, the driving characteristics at the same driving voltage, such as driving current, luminance, and efficiency, are listed in Table 1. In the SiNx layer case, the luminance and current barrier are 178.4 cd and 0.051 A for Red, 312.6 cd and 0.028 A for Green, and 69.2 cd and 0.082 A for Blue, respectively. From these results, the efficiency of white color is determined as 40.1 cd/A. In the PI-Al_2O_3 hybrid barrier nanolayer case, the luminance and current barrier are 178.3 cd and 0.051 A for Red, 322.2 cd and 0.029 A for Green, and 71.9 cd and 0.084 A for Blue, respectively. From these results, the efficiency of white color is determined as 40.4 cd/A. From the above results, the driving characteristics are similar for both barriers, which means that there is no degradation with the PI-Al_2O_3 hybrid barrier nanolayer and it is suitable for the flexible OLED display.

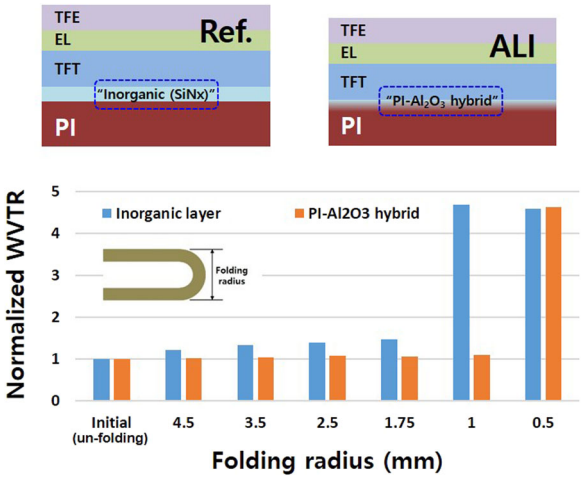

Fig. 5 The results of folding test. Flexibility test result comparison between the PI-Al_2O_3 hybrid barrier nanolayer and the inorganic layer: **a** folded characteristics; **b** normalized WVTR results according to folding radius after folding tests.

In conclusion, this work investigates ALI technology for PI-Al_2O_3 hybrid barrier nanolayer fabrication for flexible OLED displays. From the results of TEM, SIMS, GC-MS, and WVTR analysis, the PI-Al_2O_3 hybrid nanolayer is well formed in the PI layer and shows good barrier performance under optimal process conditions. In addition, the folding properties are improved when the PI-Al_2O_3 hybrid barrier nanolayer is applied. Even after 1,000 h storage testing the flexible OLED display at high-temperature and humidity, there were no dark spots and the flexible OLED display with the PI-Al_2O_3 hybrid barrier nanolayer demonstrates normal

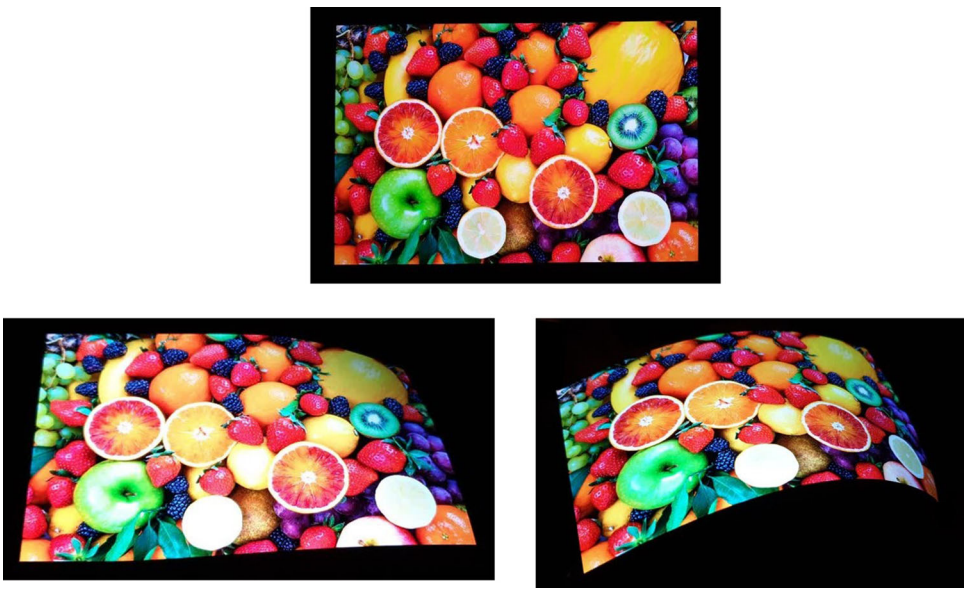

Fig. 6 Panel driving characteristics. Driving test of flexible OLED display with the PI-Al_2O_3 hybrid barrier nanolayer via ALI technology (Image from www.shutterstock.com).

Table 1. Driving characteristics of flexible OLED display with SiNx barrier layer and the PI-Al_2O_3 hybrid barrier nanolayer.

Barrier type	Red		Green		Blue		White
	Luminance (cd)	Current (A)	Luminance (cd)	Current (A)	Luminance (cd)	Current (A)	Efficiency (cd/A)
SiNx	178.4	0.051	312.6	0.028	69.2	0.082	40.1
PI-Al_2O_3	178.3	0.051	322.2	0.029	71.9	0.084	40.4

driving characteristics. Based on the results obtained in this study, we conclude that ALI technology is suitable and one of the best candidates for new barrier fabrication for improving the flexibility and reliability of flexible OLED displays.

METHODS

Flexible OLED display fabrication

On the carrier glass, PI material was coated using a slit coater and cured in an oven at high temperature as a substrate. Two types of barriers, one with a silicon nitride and one with the PI-Al_2O_3 hybrid nanolayer, were formed on and in a PI substrate. The thin-film transistor for driving and the emission layer for lighting were made on substrate via various process technologies. Then, the thin-film encapsulation for protection was formed with inorganic-organic multi-layer using the PECVD and inkjet processes. Finally, the device was peeled off the glass and laminated with a protective film.

DATA AVAILABILITY

The data that support the findings of this study are available from the corresponding author upon reasonable request.

Received: 16 August 2021; Accepted: 22 February 2022;
Published online: 13 April 2022

REFERENCES

1. Jorgensen, M. et al. Stability of polymer solar cells. *Adv. Mater.* **24**, 580–612 (2012).
2. Nikiforov, M. P., Strzalka, J. & Darling, S. B. Delineation of the effects of water and oxygen on the degradation of organic photovoltaic devices. *Sol. Energy Mater. Sol. Cells* **110**, 36–42 (2013).
3. Wiemers-Meyer, S., Winter, M. & Nowak, S. Mechanistic insights into lithium ion battery electrolyte degradation – a quantitative NMR study. *Phys. Chem. Chem. Phys.* **18**, 26595–26601 (2016).
4. Shinkle, A. A., Sleightholme, A. E. S., Griffith, L. D., Thompson, L. T. & Monroe, C. W. Degradation mechanisms in the non-aqueous vanadium acetylacetonate redox flow battery. *J. Power Sources* **206**, 490–496 (2012).
5. Jabeen, N., Majid, I. & Nayik, G. A. Bioplastics and food packaging: a review. *Cogent Food Agric.* **1**, 1117749 (2015).
6. Guzman, A., Gnutek, N. & Janik, H. Biodegradable polymers for food packaging-factors influencing their degradation and certification types-A comprehensive review. *Chem. Chem. Technol.* **5**, 115–122 (2011).
7. Dahl-hansen, R. P. et al. On the effect of water-induced degradation of thin-film piezoelectric microelectromechanical systems. *J. Microelectromech. Syst.* **30**, 105–115 (2021).
8. Schaer, M., Nuesch, F., Berber, D., Leo, W. & Zuppiroli, L. Water vapor and oxygen degradation mechanisms in organic light emitting diodes. *Adv. Funct. Mater.* **11**, 116–121 (2001).
9. Uoyama, H., Goushi, K., Shizu, K., Nomura, H. & Adachi, C. Highly efficient organic light-emitting diodes from delayed fluorescence. *Nature* **492**, 234–238 (2012).
10. Malissa, H. et al. Room-temperature coupling between electrical current and nuclear spins in OLEDs. *Science* **345**, 1487–1490 (2014).
11. Gu, G., Burrows, P., Venkatesh, S., Forrest, S. R. & Thompson, M. E. Vacuum deposited, nonpolymeric flexible organic light-emitting devices. *Opt. Lett.* **22**, 172–174 (1997).
12. Gorrn, P. et al. Towards see-through displays: fully transparent thin-film transistors driving transparent organic light-emitting diodes. *Adv. Mater.* **18**, 739–741 (2006).
13. Burrows, P. E. et al. Reliability and degradation of organic light emitting devices. *Appl. Phys. Lett.* **65**, 292–2924 (1994).
14. Papadimitrakopoulos, F., Zhang, X. M. & Higginson, K. A. Chemical and morphological stability of aluminum tris(8-Hydroxyquinoline) (Alq): effects in light-emitting devices. *IEEE J. Sel. Top. Quantum Electron.* **4**, 49–57 (1998).
15. Han, Y. C., Lim, M. S., Park, J. H. & Choi, K. C. ITO-free flexible organic light-emitting diode using ZnS/Ag/MoO3 anode incorporating a quasi-perfect Ag thin film. *Org. Electron.* **14**, 3437–3443 (2013).
16. Lee, H. S., Seo, S. W., Jung, E., Chae, H. Y. & Cho, S. M. Flexible organic light-emitting diodes on a poly(3,4-ethylenedioxythiophene)/metal-grid hybrid electrode. *Appl. Phys. Express* **6**, 046503.1–046503.4 (2013).
17. Graff, G. L., Williford, R. E. & Burrows, P. E. Mechanisms of vapor permeation through multilayer barrier films: lag time versus equilibrium permeation. *J. Appl. Phys.* **96**, 1840–1849 (2004).
18. Weaver, M. S. et al. Organic light-emitting devices with extended operating lifetimes on plastic substrates. *Appl. Phys. Lett.* **81**, 2929–2931 (2002).
19. Charton, C. et al. Development of high barrier film on flexible polymer substrates. *Thin Solid Films* **502**, 99–103 (2006).
20. Lee, L. et al. Ultra gas-proof polymer hybrid thin layer. *Nano Lett.* **18**, 5461–5466 (2018).
21. Park, S. H. K. et al. Ultrathin film encapsulation of an OLED by ALD. *Electrochem. Solid-State Lett.* **8**, 21–23 (2005).
22. Choi, B. I., Nham, H. S., Woo, S. B. & Kim, J. C. Ultralow water vapor permeation measurement using tritium for OLED displays. *J. Korean Phys. Soc.* **53**, 2179–2184 (2008).
23. Yoon, K. H. et al. Extremely high barrier performance of organic-inorganic nanolaminated thin films for organic light-emitting diodes. *Appl. Mater. Interfaces* **9**, 5399–5408 (2017).
24. Patil, P. N. et al. Free volumes and gas transport in polymers: amine-modified epoxy resins as a case study. *Phys. Chem. Chem. Phys.* **18**, 3817–3824 (2016).
25. Mondal, S., Hu, J. L. & Yong, Z. Free volume and water vapor permeability of dense segmented polyurethane membrane. *J. Membr. Sci.* **280**, 427–432 (2006).
26. Hu, L., Li, M., Xu, C., Luo, Y. & Zhou, Y. A polysilazane coating protecting polyimide from atomic oxygen and vacuum ultraviolet radiation erosion. *Surf. Coat. Technol.* **203**, 3338–3343 (2009).
27. Budd, P. M., McKeown, N. B. & Fritsch, D. Free volume and intrinsic microporosity in polymers. *J. Mater. Chem.* **15**, 1977–1986 (2005).

AUTHOR CONTRIBUTIONS

S.H.K. and M.M.S. conceived the original idea and designed the research. S.H.K., S.Y.S., W.Y.S. and H.Y.C. conducted and planed the experiment and analyses. S.H.K. mainly wrote the manuscript with figures through contributions of all authors. S.Y.K. and K.H.Y. designed the experiment object and analysis methods. M.W.C. contributed to fabricate of the test samples for various measurements and the flexible OLED displays. H.J.K. carried out the TEM, SIMS, WVTR measurements and folding and lighting test.

COMPETING INTERESTS

The authors declare no competing interests.

ADDITIONAL INFORMATION

Correspondence and requests for materials should be addressed to Seung Hun Kim.

Reprints and permission information is available at http://www.nature.com/reprints

Publisher's note Springer Nature remains neutral with regard to jurisdictional claims in published maps and institutional affiliations.